Theoretical study on naphthobischalcogenadiazole conjugated polymer systems and C61 derivative as organic photovoltaic semiconductors

doi: 10.1016/j.cplett.2018.01.021

Theoretical study on naphthobischalcogenadiazole conjugated polymer systems and C61 derivative as organic photovoltaic semiconductors

Takehiro Fujita[a], Toru Matsui[a,*], Masato Sumita[a,b], Yutaka Imamura[c], and Kenji Morihashi[a]

[a]*Department of Chemistry, Graduate School of Pure and Applied Sciences, University of Tsukuba, 1-1-1, Tennodai, Tsukuba, Ibaraki 305-8571, Japan.* [b]*Center for Advanced Intelligence Project, RIKEN Nihonbashi 1-chome Mitsui Building, 15th floor, 1-4-1 Nihonbashi, Chuo-ku, Tokyo, 103-0027, Japan.* [c]*Department of Chemistry, Graduate School of Science and Engineering, Tokyo Metropolitan University, 1-1 Minami-osawa, Hachioji, Tokyo 192-0397, Japan.*

*Corresponding author, E-mail address: matsui@chem.tsukuba.ac.jp

Abstract

We investigated the charge-transfer reactions of solar cells including a quaterthiophene copolymer with naphtho-bis-thiadiazole (PNTz4T) and naphtho-bis-oxadiazole (PNOz4T) using constrained density functional theory (CDFT). According to our calculations, the high electron-transfer rate results in a highly efficient solar cell, and the stable charge-transfer state results in low energy loss. Our computations imply that the following three factors are crucial to improve the performance of semiconducting polymers: (i) large structural changes following charge-transfer, (ii) narrow band gap, and (iii) spatially delocalized lowest unoccupied molecular orbital (LUMO) of the ground state.

Keywords

density functional theory; semiconducting polymers; charge transfer; solar cells

1. Introduction

Polymer-based bulk-heterojunction solar cells (PSCs) [1] are a type of organic photovoltaic cells (OPVs). Although dye-sensitized solar cells [2] suffer from sealing defects because they utilize liquid electrolytes, PSCs are expected to function effectively as durable solid photoelectric conversion devices. The implementation of polymer films in PSCs as the charge transport material makes them superior to inorganic solar cells in terms of weight and cost. However, two key issues must be addressed before PSCs can be used in practice. The first is their low power conversion efficiency (PCE) relative to inorganic solar cells, and the second is their large energy loss (E_{loss}) [3] (0.7–0.8 eV) as solar energy is converted into electric power.

Although PSCs have several problems generating free electron–hole pairs from sunlight, one method to improve their low PCE and large E_{loss} is to effectively combine their constituent materials. PSCs consist of two types of organic semiconductors with many π electrons; that is, hole transport and electron transport materials with electron-donating and electron-accepting properties, respectively. Current PSCs are composed of polycyclic aromatic hydrocarbons or π-electron conjugated (semiconducting) polymers as the hole transport materials and fullerene derivatives as the electron transport materials. Charge recombination [4], which negatively affects charge-transfer, is assumed to be the

main cause for the low PCE of PSCs. For materials with low bulk electrical conductivity, charge recombination is attributed to unstable electron–hole pairs. Therefore, it is helpful to analyse several combinations of hole transport and electron transport materials to better understand their electronic structure.

To increase the PCE of PSCs, semiconducting polymers [5-7] have been developed in the framework of two essential aspects; one is to control the thin film structure, such as its crystallinity and orientation, so as to enhance the efficiency of charge transport, whereas the other aspect is to control the polymers' electronic structure, such as the absorption wavelength and the energy levels of the frontier orbitals, which are important for exciton formation. Regarding the electronic structure, a semiconducting polymer with a narrow band gap and deep highest occupied molecular orbital (HOMO) level is preferable to widen the absorption region and increase the open circuit voltage. Osaka *et al*. reported an effective copolymer based on quaterthiophene and naphtho-bis-thiadiazole (PNTz4T) [8], with the PCE of PNTz4T with [6,6]-phenyl-C61-butyric acid methyl ester (PCBM) (PNTz4T/PCBM) reaching more than 10%. In addition, they also reported a quaterthiophene and naphtho-bis-oxadiazole copolymer (PNOz4T) [9]. Both PNTz4T and PNOz4T have a high crystallinity, narrow band gap, and deep HOMO level. Although the PCE of the PSC with PNOz4T was relatively low (9%), PNOz4T has

received considerable attention, particularly because of its small E_{loss} (0.53–0.55 eV). Although clarifying the difference between PNTz4T/ and PNOz4T/PCBM will be helpful to develop more efficient materials, experiments are often not suitable to observe details of the charge-transfer process.

To this end, quantum chemical analyses are a powerful tool to obtain detailed understanding of charge-transfer processes. However, conventional density functional theory (DFT) struggles to describe the charge-transfer states where positive and negative charges are localized in the hole transporting and electron transporting materials. This shortcoming of several exchange–correlation DFT functionals results from self-interaction error (SIE) [10], which includes unphysical electron interactions in the energy evaluation.

Constrained density functional theory (CDFT) of Deberich *et al*. [11,12] is an effective tool for solving charge-localized systems. CDFT can minimize the energy of the system under the constraint that the charges and spins remain localized in particular regions of the system by adding a Lagrange multiplier to the conventional Kohn-Sham DFT equations. Wu *et al*. developed CDFT further by reporting a way to efficiently explore the diabatic potential energy curves in Marcus' electron-transfer theory [13], as well as a way to accurately predict the driving force and reorganization energy [14]. Indeed, using Wu's

approach, a lot of electron-transfer reactions were explained [15-17] by computing the electron-transfer rate constant within the Condon approximation [18]. Because of this success, we adopted CDFT to estimate the charge-transfer reactions in PSCs.

This study aims to understand the qualitative differences between PNTz4T and PNOz4T by comparing the electron-transfer rates (k_{ET}) and the stability of the charge-transfer state between PNTz4T/PCBM and PNOz4T/PCBM. Moreover, we also investigated the conformational dependence of these molecular species on k_{ET}.

2. Method

2.1. Modelling

In this study, we used a donor/acceptor complex extracted from the interface between bulk PCBM and PNTz4T/PNOz4T. PNTz4T or PNOz4T was adopted as the electron donor, and PCBM [19] was chosen as the electron acceptor, as in the experiments of Osaka *et al*. [9]. The PCBM model systems with PNTz4T or PNOz4T were prepared as follows. First, PNTz4T and PNOz4T were orientated face-on to PCBM at the interfaces, and the polar substituents of PCBM were directed toward the bulk region due to electrostatic repulsion. Hence, we created the donor–accepter complex models as shown in Figure 1a. The initial structures were prepared to ensure that the nearest distance

between the donor and acceptor atoms was approximately 4.0 Å. (see the SI for the detailed initial structures.) For computational convenience, PNTz4T and PNOz4T were modelled as monomers by replacing the alkyl chains with methyl groups, which are hereafter termed NTz4T and NOz4T, respectively. We found that these small model systems are sufficiently representative of the actual systems to reproduce the three relevant electronic states of the system (i.e. before light irradiation, after exciton formation, and after charge-transfer).

Additionally, we prepared six models for each NTz4T/PCBM and NOz4T/PCBM complex (Figure 2) by rotation around the C_2 axis (Figure 1b) to examine their conformational dependence on k_{ET}. These models are hereafter referred to as **s1**-**s6**. As shown in Figure 1b, PCBM was placed above the thiophene rings or the carbon–carbon bonds of NTz4T or NOz4T.

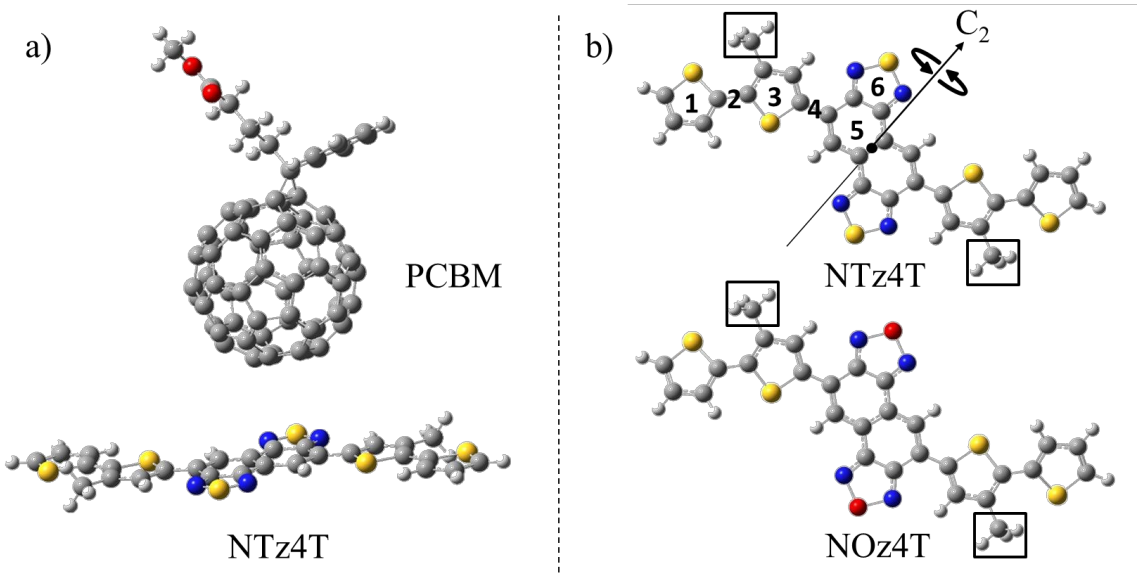

Figure 1. (a) Model of the NTz4T complex with PCBM (NTz4T/PCBM). Blue, red, yellow, white, and grey spheres indicate nitrogen, oxygen, sulfur, hydrogen, and carbon atoms, respectively. (b) Structures of NTz4T and NOz4T. PCBM is placed above the NTz4T or NOz4T moieties and labelled from **1** to **6**, as depicted as **s1**-**s6** in Figure 2. Face-on conformations were ensured by enforcing C_{2h} symmetry of NTz4T/NOz4T.

2.2. Geometry Optimization and Single-Point Energy Calculations

All calculations in this study were performed using the B3LYP [20] hybrid density functional and the 6-31G(d) basis set. The total energy of these models was determined through the following three steps: (i) all-atom geometry optimization of the ground state, (ii) geometry optimization of each molecule, and (iii) single-point energy calculations. All models were optimized using GAUSSIAN 09 [21]. Only the donor was extracted from

the optimized structures of **s1-s6**, and geometry optimizations of the singlet ground and excited states and the radical cation state were performed. Time-dependent DFT (TD-DFT) [22] as implemented in GAUSSIAN 09 was used to calculate the singlet excited state. For PCBM, geometry optimizations of the singlet ground and radical anion states were also performed. These optimized molecules were then combined while maintaining their ground-state interatomic distances. Finally, single point-energy calculations were performed using our own CDFT program [15-17]. After the charge-transfer was calculated for each system, the constraint was set to ensure charges of +1 and -1 for the donor and acceptor, respectively.

2.3. Electron Transfer Rate and Stabilization Energy

The electron-transfer rate constants, k_{ET}, were calculated using Equation (1) [23]:

$$k_{ET} = \frac{4\pi^2}{h} \frac{|H_{ab}|^2}{\sqrt{4\pi\lambda k_B T}} \exp\left(-\frac{(\Delta G^0 + \lambda)^2}{4\lambda k_B T}\right) \qquad (1)$$

where h, k_B, and T are Planck's constant, Boltzmann's constant, and absolute temperature, respectively. The driving force (ΔG^0), reorganization energy (λ), and electron coupling constant (H_{ab}) were calculated from the energy and orbitals obtained by single-point

energy calculations at the CDFT level of theory. k_{ET} was determined with T = 300 K and H_{ab} was calculated based on the theory proposed by Wu *et al*. [18]. Because CDFT struggles to describe singlet excited states, H_{ab} was approximated by assuming that the triplet excited state is equal to the singlet excited state.

Hereafter, we use the standard notation $E(a|b)$ to represent the energy in the "a" state with the equilibrium structure in the "b" state. For example, each energy of the system before light irradiation, after exciton formation, and after charge-transfer is expressed as E(DA|DA), E(D*A|D*A), and $E(D^{+\bullet}A^{-\bullet}|\ D^{+\bullet}A^{-\bullet})$, respectively. Here, D and A indicate the donor and acceptor, respectively. ΔG^0 was obtained approximately from the difference between the internal energies of the systems as follows:

$$\Delta G^0 \fallingdotseq E(D^{+\bullet}A^{-\bullet}|D^{+\bullet}A^{-\bullet}) - E(D^{*}A|D^{*}A) \qquad (2)$$

Because we assumed that the electron-transfer occurs in a gas phase, outer sphere reorganization energy due to the solvent relaxation is not taken into account. In this case, the total reorganization energy λ is equal to its inner sphere energy λ_i as:

$$\lambda = \lambda_i = E(D^{+\bullet}A^{-\bullet}|D^{*}A) - E(D^{+\bullet}A^{-\bullet}|D^{+\bullet}A^{-\bullet}) \qquad (3)$$

A stabilization energy E_{st} was introduced to assess the stability of the charge-transfer state ($D^{+\bullet}$ and $A^{-\bullet}$); larger values of E_{st} indicate higher stability of this state.

$$E_{st} = E(D^{+\bullet}|D^{+\bullet}) + E(A^{-\bullet}|A^{-\bullet}) - E(D^{+\bullet}A^{-\bullet}|D^{+\bullet}A^{-\bullet}) \qquad (4)$$

3. Results and Discussion

3.1 Structural Changes

Figure 2 shows the optimized structures of **s1**-**s6**. Relative to their initial structures, no significant changes of **s1**-**s4** were evident. However, the optimized structures of **s5** and **s6** show slightly longer distances from NTz4T and NOz4T compared with their initial structures.

Although NTz4T and NOz4T have slightly bent ground-state structures, they are almost planar in the lowest-energy singlet excited state. The geometric difference between the excited and radical cation states is not significant. Indeed, the root mean square deviation (RMSD) of all atomic coordinates of **s1-s6** is 0.0155 Å for NTz4T and 0.0167 Å for NOz4T. Additionally, there was little structural difference between the ground state of PCBM and its radical anion.

We also calculated λ_{NTz4T}, λ_{NOz4T}, and λ_{PCBM} to evaluate the contribution of the reorganization energy to the stability of the entire system. The respective average values of all conformations (**s1**-**s6**) are $\overline{\lambda_{\mathrm{NTz4T}}}$ = 8.38 kJ/mol, $\overline{\lambda_{\mathrm{NOz4T}}}$ = 9.06 kJ/mol, and $\overline{\lambda_{\mathrm{PCBM}}}$ = 12.71 kJ/mol. Clearly, PCBM contributes the most to the total reorganization energy, and NOz4T has a slightly larger contribution than NTz4T.

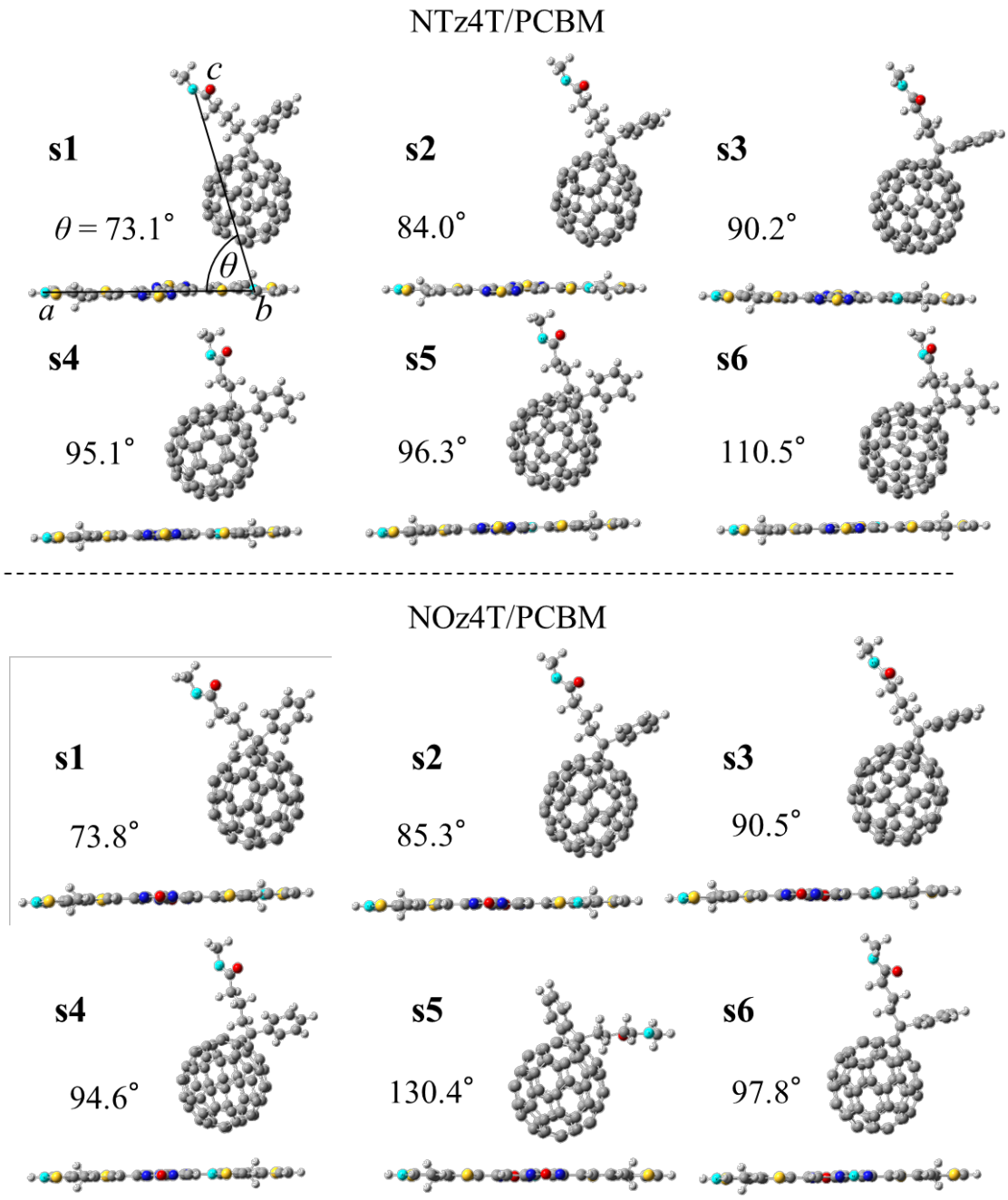

Figure 2. Fully optimized structures of **s1-s6**. The nearest intermolecular distance between the donor and acceptor atoms is almost identical to that of the initial structure. The angles (θ) between the cyan-coloured *a*, *b*, and *c* atoms are shown. *a*: terminal carbon atom of the NTz4T or NOz4T ring. *b*: nearest atom to PCBM. *c*: ether bonding

oxygen atom of PCBM. **s5** of NOz4T/PCBM has an especially large angle because the orientation of the functional groups of PCBM is reversed.

3.2 Absorption Wavelengths and Molecular Orbitals

We compared the absorption wavelengths (γ) of NTz4T and NOz4T at the TD-DFT level of theory with the experimental values [9] to examine whether the singlet excited state corresponds to the actual system. According to our calculations, the first transition-allowed excited state could be attributed to a single electron excitation from the HOMO to the lowest unoccupied molecular orbital (LUMO) of NTz4T and NOz4T (Figure 3). Although the computed absorption wavelength was slightly shorter than the experimental value (<50 nm), because of the short-conjugated monomer model [24], the tendency is consistent with experimental results; that is, NTz4T has a shorter absorption wavelength and weaker oscillator strength than NOz4T [9]. It is expected that excitation of NOz4T occurs more efficiently than that of NTz4T because the oscillator strength of the HOMO–LUMO excitation of NOz4T is larger than that of NTz4T (Figure 3).

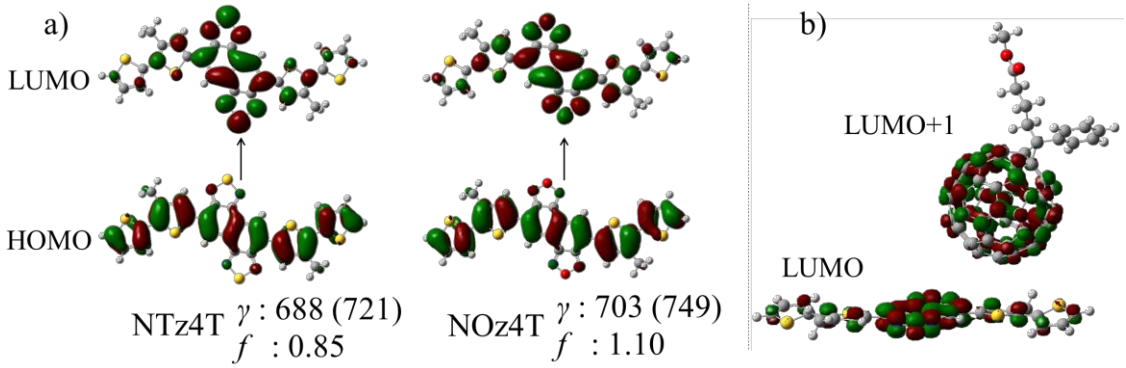

Figure 3. (a) HOMO/LUMO of NTz4T and NOz4T (isovalue of 0.020). The values of γ are given in nm, and the experimental values are shown in parentheses. The values of the absorption oscillator strength (f) are also given. (b) LUMO and LUMO+1 of NOz4T/PCBM (isovalue of 0.020), which are almost degenerate (<5 kJ/mol).

3.3 Calculated k_{ET} and E_{st}

Table 1 shows the k_{ET} and E_{st} of the systems and the three Marcus parameters. The overlap integrals between the donor and acceptor are shown in parentheses as a supplement to H_{ab}. For clarity, the qualitative differences of these were considered. Although efficient charge-transfer is expected in both models on the basis of k_{ET}, the NTz4T/PCBM model has a relatively larger k_{ET} than that of NOz4T/PCBM. These results reflect the high efficiency of PSCs using PNTz4T. Since the right-hand side of Eq. (1) contains $(\Delta G^0 + \lambda)^2$ in the exponential term, the k_{ET} difference between the models is mainly due to the difference between ΔG^0 and λ. The average ΔG^0 values in **s1**-**s6** in the

NTz4T/PCBM and NOz4T/PCBM models are -70.71 and -85.21 kJ/mol, respectively. As for the average λ in **s1-s6**, we obtain 16.72 kJ/mol for NTz4T/PCBM and 19.76 kJ/mol for NOz4T/PCBM. From these results, this reaction occurs in the inverted region of Marcus theory for both models, and the large k_{ET} of NTz4T/PCBM is attributed to its small $(\Delta G^0 + \lambda)^2$ value.

Moreover, the k_{ET} values of **s4-s6** in NTz4T/PCBM tend to be much larger than those in **s1-s3**, indicating that k_{ET} is conformation dependent. The primary difference between **s4-s6** and **s1-s3** is attributed to the difference in H_{ab}; H_{ab} for **s4-s6** are ~100 times larger than those of **s1-s3**. Therefore, we can speculate that conformation contributes to H_{ab}, which increases when the donor and acceptor couple strongly. The strength of the coupling between the donor and acceptor is reflected in the value of the overlap integral, which is increased when the MOs of the donor and acceptor are closer. Indeed, as shown in Figure 3, the LUMOs in the ground state of NTz4T and NOz4T are localized in the naphtho-bis-thiadiazole (NTz) and naphtho-bis-oxadiazole (NOz) moieties, and PCBM in **s4-s6** is in the proximity of these orbitals. Therefore, the overlap integral becomes large (Table 1), and strong coupling occurs between the donor and acceptor.

Although the same tendency is found in **s4-s6** of NOz4T/PCBM, the reorganization energy has an important contribution to the large k_{ET} in **s5** and **s6**. In addition, the

calculated coupling constant for **s5** is very small. Structurally, PCBM is out of the ring plane from the first step of the geometry optimization (Figure 4). The structural specificity of **s5** can also be ascertained from its relatively large angle involving PCBM and its counterpart (Figure 2). Although it differs from the assumed conformation, we can gauge the magnitude of the contribution of λ by comparing **s5** with **s1-s3**.

The average value of E_{st} for the NTz4T/PCBM system (136.94 kJ/mol) is smaller than that of NOz4T/PCBM (143.28 kJ/mol). This result suggests that the large E_{st} could be a factor for lowering E_{loss}. E_{loss} is defined as E_g–eV_{OC}, where E_g is the bandgap, e is the elementary charge, and V_{OC} is the open-circuit voltage. E_{st} is a value derived using the total energy of the system, whereas E_{loss} is a value derived using the bandgap; comparing these two values directly is therefore questionable. Nevertheless, the values of E_g as derived from γ are 1.80 eV for PNTz4T and 1.76 eV for PNOz4T, which do not differ considerably from the experimental values [9]. Although there is no research that reports the correlation between E_{st} and E_g, or E_{st} and E_{loss}, these properties could have a negative correlation with each other. We intend to confirm the correlation between E_{st} and E_g, and subsequently E_{st} and E_{loss}, in future studies by increasing the number of calculation targets.

Consistent with our expectations, **s4** and **s5** of NTz4T/PCBM have larger E_{st} values than

those of NOz4T/PCBM, because NTz4T has a large overlap integral with PCBM in these conformations. The same tendency is also observed in **s4** of NOz4T/PCBM.

Table 1. Calculated values of ΔG^0, λ, $|H_{ab}|$, k_{ET}, and E_{st}, with the overlap integral between NTz4T/NOz4T and PCBM in parentheses.

	s1	**s2**	**s3**	**s4**	**s5**	**s6**
NTz4T/PCBM						
ΔG^0 [a]	-79.44	-78.35	-77.39	-55.95	-60.23	-72.87
λ [a]	15.52	15.43	16.11	18.77	15.52	18.95
$\|H_{ab}\|$ [a]	0.49 (0.006)	0.14 (0.002)	0.43 (0.006)	17.76 (0.167)	16.24 (0.149)	10.70 (0.095)
k_{ET} [b]	6.65×10^{0}	1.08×10^{0}	1.03×10^{2}	1.42×10^{12}	2.53×10^{11}	1.73×10^{8}
E_{st} [a]	133.23	135.26	136.05	155.85	154.09	143.23
NOz4T/PCBM						
ΔG^0 [a]	-86.23	-88.84	-86.27	-80.66	-86.39	-82.89
λ [a]	16.09	19.59	16.30	15.69	25.05	25.85
$\|H_{ab}\|$ [a]	0.42 (0.012)	0.09 (0.001)	0.15 (0.008)	12.36 (0.095)	0.56 (0.007)	9.13 (0.077)
k_{ET} [b]	6.67×10^{-2}	1.18×10^{0}	1.56×10^{-2}	2.34×10^{3}	5.74×10^{5}	1.95×10^{9}
E_{st} [a]	142.41	139.41	142.39	149.50	141.11	144.87

[a] kJ/mol. [b] s^{-1}.

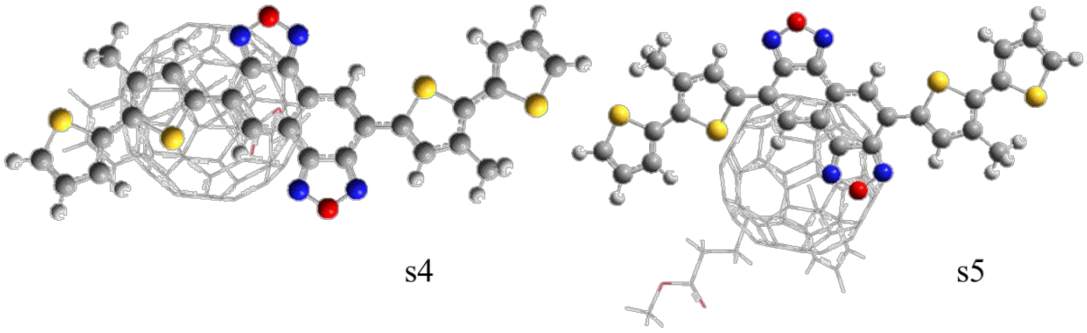

Figure 4. Structures of **s4** and **s5** (NOz4T/PCBM) viewed from the side of NOz4T. NOz4T and PCBM are depicted by ball-and-stick and wireframe styles, respectively.

3.4 Discussion

Osaka *et al*. [9] have estimated that the driving force for the electron-transfer reaction at the PNOz4T/PCBM interface is ~12 kJ/mol on the basis of the energy gap between the LUMO of the donor and acceptor (ΔE_L). Its corresponding PCE is ~9%, which implies that this reaction is efficient. However, the driving force of 12 kJ/mol is smaller than the empirically known threshold value [25] of 0.30 eV (~30 kJ/mol) for efficient electron-transfer, indicating that the PNOz4T/PCBM interface is an exception to the rule suggested in Ref. 25. In this study, the driving force at the PNOz4T/PCBM interface was estimated by using the total energy of the system, and a sufficient driving force was attained even in the PSC using PNOz4T.

The results show that a semiconducting polymer with a high PCE has a large k_{ET} and that

a small energy loss has a large E_{st}. Therefore, a semiconducting polymer with an improved PCE and small E_{loss} has both a large k_{ET} and E_{st}.

λ and ΔG^0 contribute greatly in determining the magnitude of k_{ET}. Since the sum of λ and ΔG^0 is negative, the reactions assumed in this study occur in the Marcus inverted region. Here, k_{ET} increases with an increase of λ or a decrease of $|\Delta G^0|$ (Figure 5). Because the correlation between ΔG^0 and λ is relatively weak, we conclude that these parameters are mutually independent. In contrast, ΔG^0 and E_{st} are correlated through the energy of the charge-transfer state $E(D^{+\bullet}A^{-\bullet}|\ D^{+\bullet}A^{-\bullet})$. Therefore, semiconducting polymers should be designed by focusing on lowering the energy of the lowest-energy singlet excited state E(D*A|D*A) to decrease the absolute value of ΔG^0 without affecting E_{st}; that is, semiconducting polymers with a narrow bandgap are preferable. However, polymers that experience large structural changes before and after charge-transfer should be considered to increase λ.

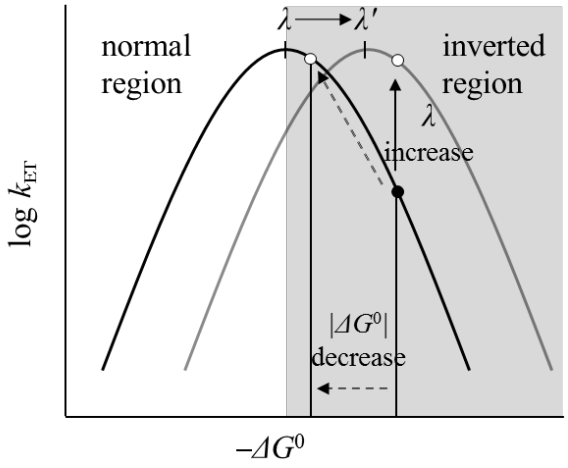

Figure 5. Conceptual diagram of the Marcus curve. Solid and dotted arrows represent the direction of the λ increase and $|\Delta G^0|$ decrease, respectively. The filled and open dots indicate plots of the actual and ideal systems, respectively.

To improve E_{st}, increasing the contribution of charge delocalization (i.e. expanding the π-conjugated system) seems to be effective. Because E_{st} also tends to increase as H_{ab} increases, it is also conceivable to design a semiconducting polymer with a spatially delocalized LUMO in the ground state.

4. Conclusion

This study investigated the electron-transfer rate constant (k_{ET}) by Marcus theory and the stabilization energy of the charge-transfer state (E_{st}) for each conformation of the NTz4T/PCBM and NOz4T/PCBM models at the CDFT level. A high PCE is predicted

for NTz4T/PCBM with a large k_{ET}, and NOz4T/PCBM with a large E_{st} has a small E_{loss}.

In the **s4**-**s6** conformations where PCBM exists above the NTz and NOz moieties, the LUMO in the ground state of the donor has a large overlap integral with the acceptor, resulting in a large k_{ET}. Therefore, we found that NOz and NTz, as introduced into a semiconducting polymer by Osaka *et al*., greatly contribute to enhancing the efficiency of electron-transfer.

It was also found that the PSC based on PNOz4T possesses a satisfactory driving force for electron-transfer, as estimated from the total energy of the system. Overall, our computational results support the high efficiency of PSCs based on PNOz4T, and the scheme introduced by Wu *et al*. is applicable for estimating electron-transfer reactions in PSCs. We expect that their scheme is effective to the electron-transfer reactions of other PSC systems as well.

In order to develop semiconducting polymers with effectual PCE and small E_{loss}, it is necessary to increase the magnitudes of both k_{ET} and E_{st}. The requirements to improve the performance of semiconducting polymers include: (i) large structural changes through charge-transfer to enhance λ, (ii) narrow band gap to lower the driving force, and (iii) spatially delocalized LUMO of the ground state to increase electronic coupling.

Acknowledgements

This study was supported by Grants-in-Aid for Scientific Research (B) (No. 17H03034) from the Japanese Society for the Promotion of Science (JSPS). Some calculations were performed at the Research Center for Computational Science (RCCS), Okazaki Research Facilities, and National Institutes of Materials Sciences (NIMS).

References

[1] I. Osaka, M. Shimawaki, H. Mori, I. Doi, E. Miyazaki, T. Koganezawa, K. Takimiya, J. Am. Chem. Soc. 134 (2012) 3498.

[2] B. Liu, E. S. Aydil, J. Am. Chem. Soc. 131 (2009) 3466.

[3] M. Wang, H. Wang, T. Yokoyama, X. Liu, J. Am. Chem. Soc. 136 (2014) 12576.

[4] A. Pivrikas, N. S. Sariciftci, G. Juska, R. Osterbacka, Prog. Photovolt: Res. Appl. 15 (2007) 677.

[5] G. Yu, J. Gao, J. C. Hummelen, Science 270 (1995) 1789.

[6] A. Facchetti, Mater. Today 16 (2013) 123.

[7] Y. Liang, Z. Xu, J. Xia, Adv. Mater. 22 (2010) 135.

[8] V. Vohra, K. Kawashima, T. Kakara, T. Koganezawa, I. Osaka, K. Takimiya, H. Murata, Nat. Photonics 9 (2015) 403.

[9] K. Kawashima, Y. Tamai, H. Ohkita, I. Osaka, and K. Takimiya, Nat. Commun. 6 (2015) 10085.

[10] I. Ciofini, C. Adamo, H. Chermette, Chem. Phys. 309 (2005) 67.

[11] P. H. Dederichs, S. Blugel, R. Zeller, H. Akai, Phys. Rev. Lett. 53 (1984) 2512.

[12] B. Kaduk, T. Kowalczyk, and T. V. Voorhis, Chem. Rev. 112 (2012) 321.

[13] R. A. Marcus, J. Chem. Phys. 24 (1956) 966.

[14] Q. Wu, T. V. Voorhis, J. Phys. Chem. A 110 (2006) 9212.

[15] T. Ogawa, M. Sumita, Y. Shimodo, K. Morihashi, Chem. Phys. Lett. 511 (2011) 219.

[16] K. Aikawa, M. Sumita, Y. Shimodo, K. Morihashi, Phys. Chem. Chem. Phys. 17 (2015) 20923.

[17] K. Aikawa, T. Matsui, K. Morihashi, Chem. Lett. 45 (2016) 628.

[18] Q. Wu, T. V. Voorhis, J. Chem. Phys. 125 (2006) 164105.

[19] J. C. Hummelen, B. W. Knight, F. LePeq, F. Wudl, J. Org. Chem. 60 (1995) 532.

[20] A. D. Becke, J. Chem. Phys. 98 (1993) 5648.

[21] GAUSSIAN 09, Revision D. 01, M. J. Frisch, *et al*., Gaussian Inc. Wallingford CT, 200

[22] E. Runge, E. K. U. Gross, Phys. Rev. Lett. 52 (1984) 997.

[23] R. A. Marcus, N. Sutin, Biochem. BioPhys. 811 (1985) 265.

[24] T. Matsui, Y. Imamura, I. Osaka, K. Takimiya, T. Nakajima, J. Phys. Chem. C 120 (2016) 8305.

[25] M. C. Scharber, D. Muhlbacher, M. Koppe, Adv. Mater. 18 (2006) 789.